SUPPLEMENTARY MATERIAL

Methods

U-Pb dating by LA-ICPMS

In-situ dating by laser ablation inductively coupled plasma mass spectrometry (LA-ICPMS) was carried out using an Element XR sector-field ICP-MS interfaced to an UP-193FX ArF excimer laser ablation system at the Institute of Earth Sciences of the University of Lausanne. The mass spectrometer was optimized according to Ulianov et al. (2012). A soft ablation regime including a repetition rate of 5 Hz and an on-sample energy density of 2.3 J/cm^2 was applied to minimize the laser-induced fractionation; pit sizes were 35 μm in diameter. The GJ-1 zircon standard was used as a primary standard for the mass bias calibration (ID-TIMS $^{206}Pb/^{238}U$ age of 600.4±0.6 Ma; Schaltegger et al., unpublished). The Harvard 91500 zircon standard (Wiedenbeck et al., 1995) was employed as a secondary standard to monitor the age accuracy during the analytical drift. Raw data were reduced using the LAMTRACE software (Jackson, 2008). No common lead correction was applied due to the presence of ^{204}Hg in the system; a qualitative count rate control on masses 201 and 204, as well as a control of cathodoluminescence images were practiced to discard analyses containing a non-negligible amount of common lead (Jackson et al., 2004).

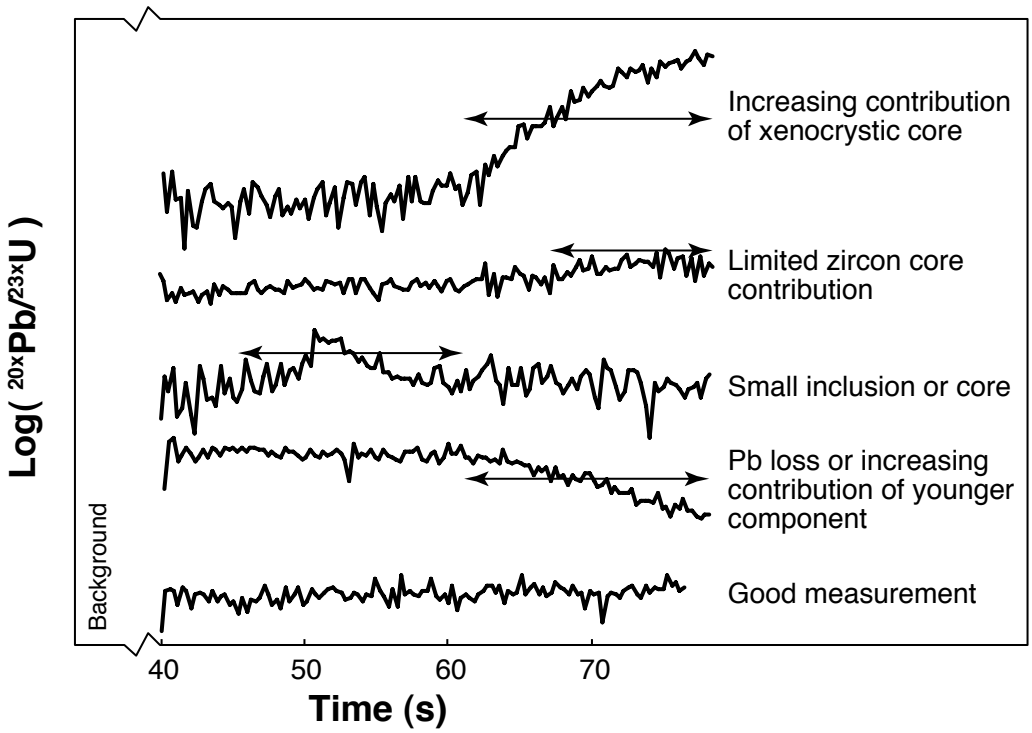

Figure A1: Examples time resolved $^{206}Pb/^{238}U$ or $^{207}Pb/^{235}U$ LA-ICPMS spectra showing the different types of heterogeneous signal encountered during zircon analysis. Only the measurements that display isotopic homogeneity similar to the bottom example are reported in the present study.

The isotopic homogeneity of the ablated material was consistently monitored on the time resolved $^{206}Pb/^{238}U$ and $^{207}Pb/^{235}U$ spectra. Analyses with changing or fluctuating ratios (Figure A1) with time were interpreted as reflecting mixing between different age domains or isotopic disturbance (lead loss, common lead, partial dissolution and recrystallization) and were discarded. Reported errors (ESM B) consist of analytical uncertainties only and do not include uncertainties on the reproducibility of the measurements on the primary nor secondary standards (~1% on primary standard).

Trace element analysis by LA-ICPMS

Trace element abundances in zircon were analyzed by LA-ICPMS using the same instrument as for U-Pb dating. The mass spectrometer optimization was similar to that described by (Ulianov et al., 2012). Operating conditions of the ablation system included a repetition rate of 5 Hz, a pit size of 25 μm and an on-sample energy density of 3.0 J/cm^2. The standard glass SRM 612 from NIST was employed for external standardization. Si^{29} served as an internal standard. Raw data were reduced using the LAMTRACE software (Jackson, 2008).

U-Pb dating by CA-ID-TIMS

Zircons were analyzed as single grain by ID-TIMS at the University of Geneva following procedure described in Schoene et al. (2010) and Wotzlaw et al. (2013). Prior to dissolution grains were individually annealed at 900 °C for 48 h in a muffle furnace, transferred into 3 ml Savillex beakers and chemically abraded in HF + trace HNO_3 at 180 °C for 15 h in Parr bombs. Zircons were subsequently rinsed individually with water, fluxed for several hours in 6 N HCl and ultrasonically cleaned with water and 3 N HNO_3. Only 4 grains from sample 11CC01 and 5 grains from sample 10CC56 that were not previously mounted on epoxy, were hand-picked, annealed and leached collectively for each sample. Single crystals were loaded in 200 μl Savillex capsules, spiked with 4–12 mg of the EARTHTIME ^{202}Pb-^{205}Pb-^{233}U-^{235}U tracer solution (ET2535, http://www.earth-time.org/) and dissolved in 70 μl HF and traces of HNO_3 at 210 °C for 60+ h in Parr bombs, dried down and redissolved in 6N HCl overnight. Samples were then dried down again and redissolved in 3N HCl and put through a modified single 50 μl column anion exchange chemistry (Krogh, 1973). The Zr, Hf, and trace element fraction (‘‘wash’’) was collected for Hf isotope analyses (see below). The U–Pb fraction was loaded on outgassed Re filaments with a Si-Gel emitter modified from (Gerstenberger and Haase, 1997). U and Pb isotopic measurements were performed on a Thermo TRITON thermal ionization mass spectrometer. Pb was measured in dynamic mode on a MasCom secondary electron multiplier. Analyses were corrected using the fractionation factor derived from the measured $^{202}Pb/^{205}Pb$ ratio assuming a true value of 0.99924. Most U was measured as U-oxide in static mode on Faraday cups equipped with 10^{12} Ω resistors. Low-U samples were measured in

dynamic mode on a MasCom secondary electron multiplier. Measured isotopic ratios were corrected for interferences of $^{233}U^{18}O^{16}O$ on $^{235}U^{16}O_2$ using an $^{18}O/^{16}O$ of 0.00205, measured on large U500 loads, and for mass fractionation using the measured $^{233}U/^{235}U$ ratio relative to a value of 0.99506 for the tracer and assuming a sample $^{238}U/^{235}U$ ratio of 137.818 ± 0.045 (2σ, Hiess et al., 2012). The SEM deadtime was determined and monitored periodically by measurements of SRM981, SRM982 (for Pb), and U500 (for U) reference materials and was found to be constant up to 1.3 Mcps but different for Pb (23 ns) and U (22 ns). All common Pb in the zircon analyses (average: 0.60 ± 0.17 pg, 1SD) was assumed to be procedural blank ($^{206}Pb/^{204}Pb$ = 18.30 ± 0.13, $^{207}Pb/^{204}Pb$ = 15.59 ± 0.16, $^{208}Pb/^{204}Pb_i$ = 37.60 ± 0.37; 1SD). U–Pb ratios and dates were calculated relative to a $^{235}U/^{205}Pb$ ratio of 100.23 ± 0.023% (1σ) and raw data were reduced using Tripoli and U–Pb_Redux software (Bowring et al., 2011). The $^{206}Pb/^{238}U$ ratios where corrected for initial Th disequilibrium using the average Th/U ratio of several samples of the corresponding host rock. The Th/U ratio used for correction was close to 3 (from 2.8 to 3.2). All uncertainties are reported at the 95% confidence level and exclude systematic uncertainties associated with tracer calibration and decay constants. The accuracy of the data was assessed by repeated analysis of the international R33 standard zircon (Black et al., 2004), which was pre-treated by annealing–leaching and measured at an average $^{206}Pb/^{238}U$ age of 419.58 ± 0.05 Ma (N = 22; MSWD = 1.5). In addition, repeat analyses of 100 Ma synthetic solutions (Condon et al., 2008; http://www.earth-time.org) yielded an external reproducibility of $^{206}Pb/^{238}U$ date better than 0.05%.

Duration of magmatic processes or time interval between successive intrusions are calculated by difference of the appropriate $^{206}Pb/^{238}U$ zircon dates and uncertainties are propagated by quadratic addition.

Hf isotopes by MC-ICPMS

Hafnium isotopic ratios of a subset of ID-TIMS U-Pb dated zircons were analyzed employing the new Thermo NEPTUNE *plus* multicollector–ICPMS at the Department of Earth Sciences, University of Geneva. Analytical protocols were similar to those described in Wotzlaw et al. (2012; 2013). The Zr-Hf and trace element solutions collected during anion exchange chemistry were re-dissolved in ~300 µl 2% HNO_3 + trace HF and transferred into pre-cleaned autosampler PFA microtubes. The solutions were introduced into the plasma employing an Aridus desolvation nebulizer with a nominal uptake rate of 50 µl/min. Isotopic ratios were measured in static mode on Faraday detectors equipped with 10^{11} Ω resistors. ^{172}Yb, ^{173}Yb and ^{175}Lu were measured to correct for isobaric interferences of Yb and Lu on mass 176 with a $^{176}Yb/^{173}Yb$ ratio of 0.79513 (measured on Yb-doped JMC475 standard solution with various Yb/Hf) and a $^{176}Lu/^{175}Lu$ ratio of 0.02656. Yb and Hf isotopic ratios were corrected for mass fractionation by normalizing to $^{172}Yb/^{173}Yb$ of 1.35351 and $^{179}Hf/^{177}Hf$ of 0.7325 using an exponential law. Mass fractionation of Lu was assumed

to follow that of Yb. Accuracy and reproducibility of this protocol were assessed by repeat analyses of 40 ppb JMC475 standard solutions ($^{176}Hf/^{177}Hf = 0.282154 \pm 0.000008$ (corresponding to ± 0.06 epsilon unit), 2σ, n = 200). All $^{176}Hf/^{177}Hf$ ratios of unknowns were normalized to a $^{176}Hf/^{177}Hf$ of 0.282160 for JMC475. Initial $^{176}Hf/^{177}Hf$ ratios and $\varepsilon Hf_{(T)}$ were calculated using the $^{206}Pb/^{238}U$ date of the respective crystal and the CHUR parameters of Bouvier et al. (2008, $^{176}Lu/^{177}Hf = 0.0336$; $^{176}Hf/^{177}Hf = 0.282785$). All uncertainties are given at the 2σ level and include the long-term reproducibility of the JMC475 solution propagated by quadratic addition.

Xenocrystic core influence on single grain U-Pb dating by CA-ID-TIMS

Here we modeled whole grain $^{206}Pb/^{238}U$ and $^{207}Pb/^{235}U$ ratios of zircon material crystallized at 35.657 Ma over a Triassic xenocrystic core (244.15 Ma) of variable relative size. Uncertainties of the $^{206}Pb/^{238}U$ and $^{207}Pb/^{235}U$ ratios are 0.1 % and 1 % respectively, typical of CA-ID-TIMS U-Pb dating on zircons. U content of the core and the overgrowth are set to be equal. The volume of the core is modeled as a sphere while the volume of the zircon in modeled as a cylinder terminated by two cones. Results show that in these conditions, single grain CA-ID-TIMS dating would yield concordant dates for a relative xenocrystic core size up to ca. 5 vol.% (Figure A2). This simulation shows that in the absence of external constrains, a spread in zircon date of ca. 10 Ma may not represent protracted zircon crystallization over this period but rather mixed dates of variable amount of core and overgrowth.

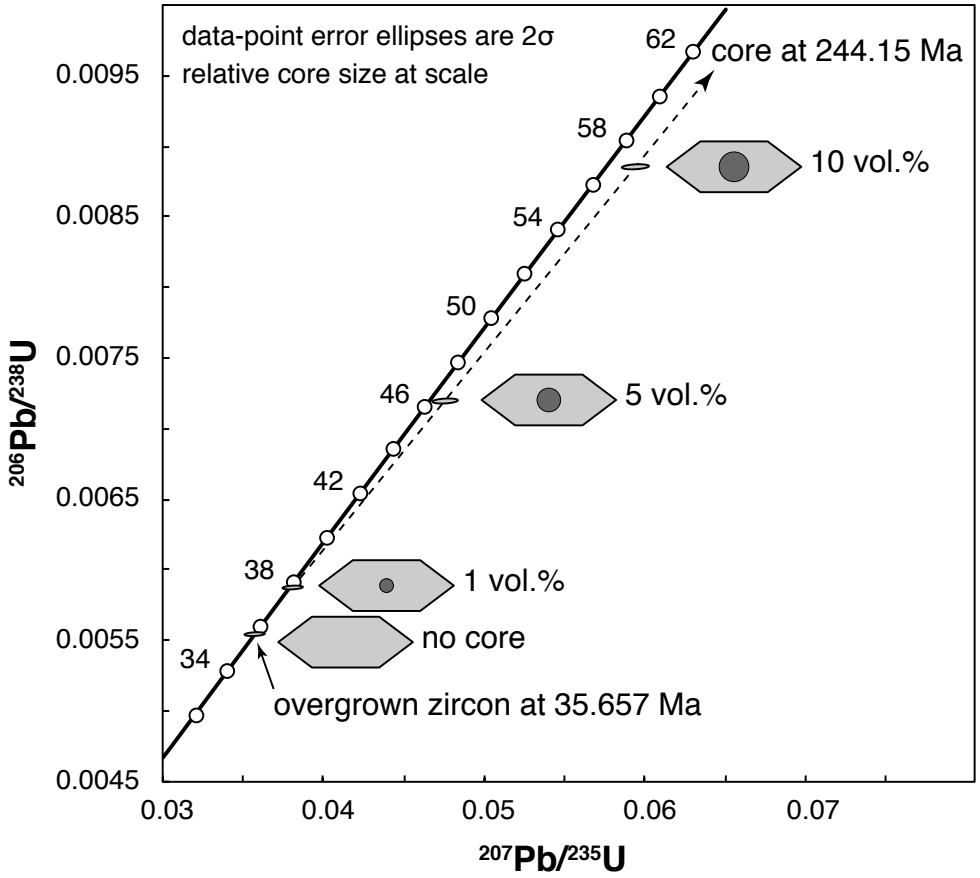

Figure A2: Synthetic Concordia plot showing the effect of Triassic xenocrystic core size with an Eocene overgrowth on whole grain ID-TIMS dating. U content of zircon core and overgrowth are set to be equal and relative precision is 0.1 % for $^{206}Pb/^{238}U$ and 1 % for $^{207}Pb/^{235}U$. Relative volume of core and overgrown zircon are at scale. The Pb/U isotopic ratios remain concordant for grain comprising up to ~5 vol.% of xenocrystic core.

Thermal modeling

First order thermal modeling was carried out in order to test the pertinence of a multimillion-year long-lived thermal anomaly as suggested by zircon dates and Hf isotopes. Crustal thermal conditions in response of ca. 2 Ma of incremental magma injections are modeled for conductive heat transfer using the HEAT3D (Wohletz, 2008) software. Input parameters are:

- Geothermal gradient = 25 °C/km
- Specific heat capacity (magma and crust) = 1200 J/kg/°C
- Thermal conductivity (magma and crust) = 2.5 W/m/°C
- Crustal rock density = 2300 kg/m^3
- Input magma temperature = 900°C

Magma injection timing was set to match the zircon record at Coroccohuayco between 37.5 Ma and 35.6 Ma with increments of 0.1 Ma. The system was then allowed to cool until 35.1 Ma. In the absence of any data on the magma flux rate and pluton volume below the Coroccohuayco deposit, we modeled two different cases. The first one was set to model the incremental assembly of a ca. 500 km^3 pluton corresponding to a long-term average magma flux of ~ $2.6 \cdot 10^{-4}$ km^3/a. The second model was set to simulate the assembly of a ca. 2100 km^3 pluton corresponding to a long-term average magma flux of ~ $1.0 \cdot 10^{-3}$ km^3/a. These magma fluxes and pluton volumes are in the range magmatic systems elsewhere (e.g. de Saint Blanquat et al., 2011) and may resemble plutons size below porphyry systems (e.g. Dilles and Proffett, 1995; Steinberger et al., 2013). Overall, increasing volumes of magma were injected every 0.1 Ma at depth between 5 and 9 km according to the proposed model for the Coroccohuayco magmatic system. The detailed magma injection scenario is presented Table A1.

Results of the thermal modeling are present Figure A3 and A4. Both models show that repetitive magma injections were able to build a stable and long-lived thermal anomaly in the upper crust. Taking for reference the temperature at 5 km depth which is ~150 °C before any magmatic activity, it yields ~270 °C and 450 °C at peak thermal conditions (35.6 Ma) for model 1 and 2, respectively. Interestingly 0.5 Ma after magmatic activity has ceased, the thermal anomaly is still prominent above the crystalline pluton (220 °C and 300 °C at 5 km for model 1 and 2, respectively).

Table A1: Magma injection scenario for thermal models 1 and 2.

Date (Ma)	Model 1	Model 2
	input magma volume (km^3)	
37.5	-	-
37.4	10	10
37.3	10	20
37.2	10	50
37.1	-	-
37.0	-	-
36.9	-	-
36.8	-	-
36.7	-	-
36.6	10	10
36.5	10	20
36.4	10	20
36.3	10	50
36.2	20	100
36.1	50	150
36.0	50	200
35.9	-	-
35.8	10	100
35.7	50	200
35.6	120	500
35.5	150	700
35.4	-	-
35.3	-	-
35.2	-	-
35.1	-	-
SUM	**520**	**2130**

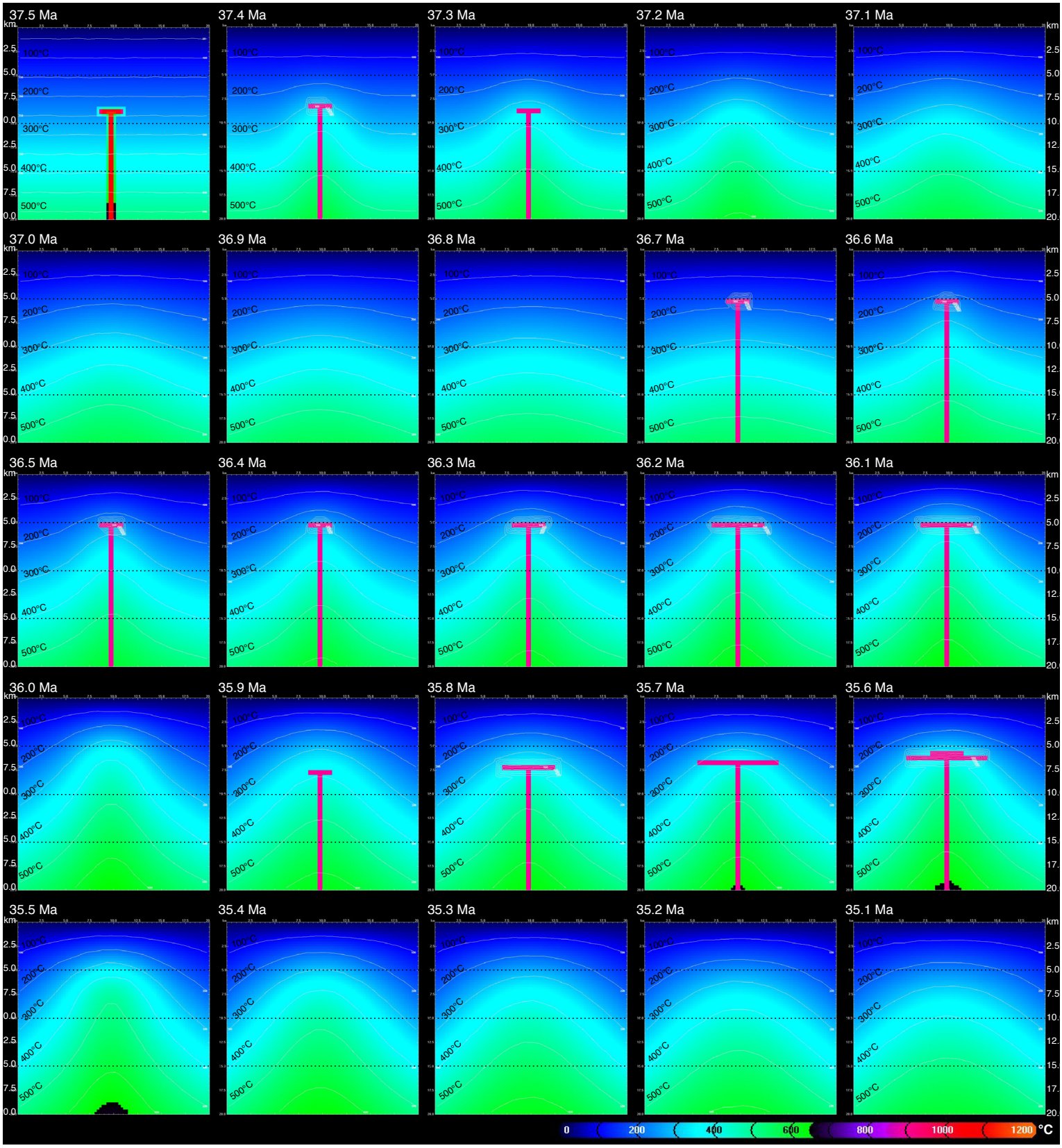

Figure A3: Thermal modeling outputs. Model 1, a total of 500 km^3 of magma is injected. Snapshots are taken every 0.1 Ma and represent the thermal conditions in the crust at a given time and the new magma batches (pink) for which shapes and sizes are defined.

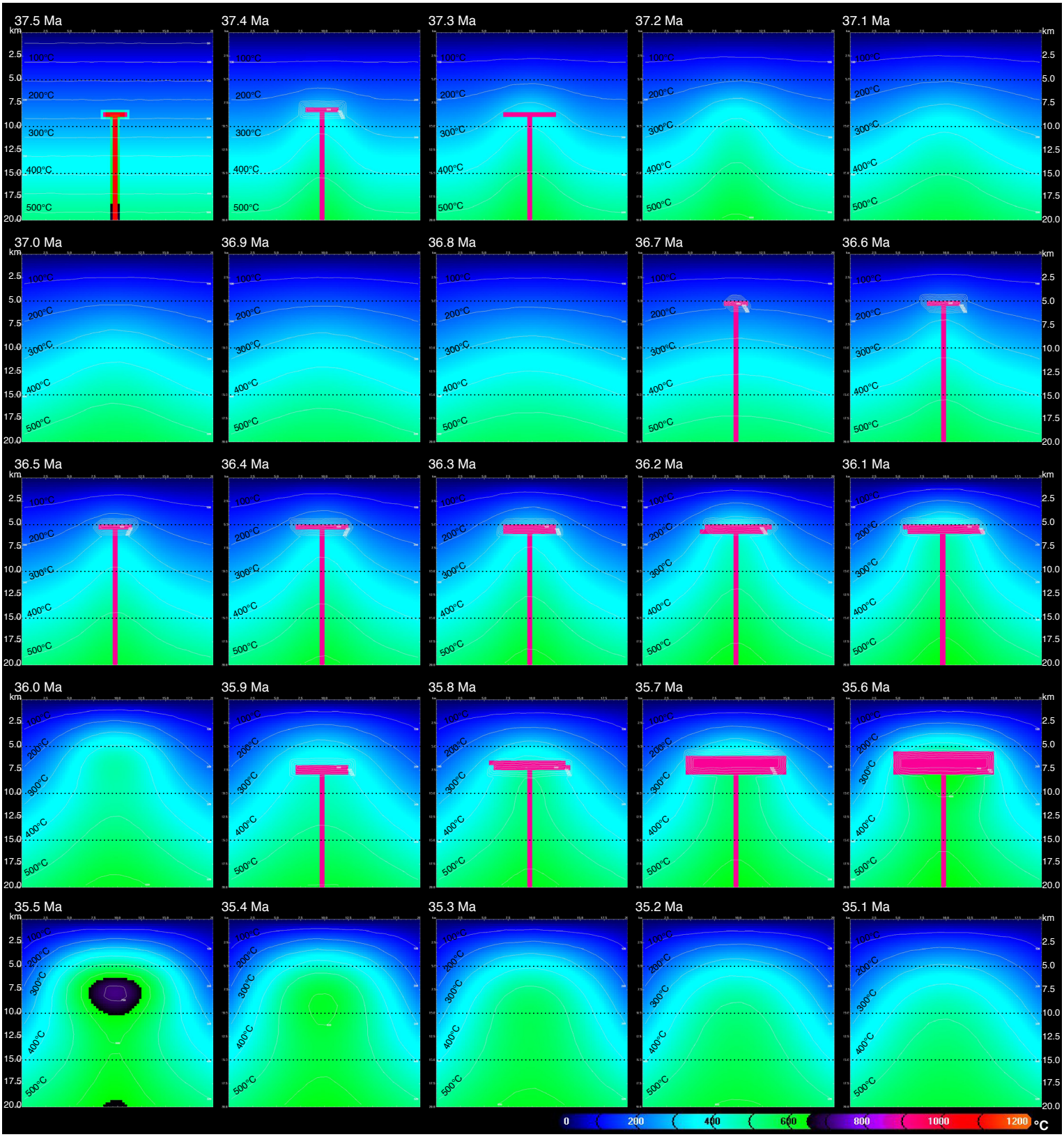

Figure A4: Thermal modeling outputs. Model 2, a total of 2100 km^3 of magma is injected. Snapshots are taken every 0.1 Ma and represent the thermal conditions in the crust at a given time and the new magma batches (pink) for which shapes and sizes are defined.

References

Black, L.P., Kamo, S.L., Allen, C.M., Davis, D.W., Aleinikoff, J.N., Valley, J.W., Mundil, R., Campbell, I.H., Korsch, R.J., Williams, I.S., Foudoulis, C., 2004. Improved $^{206}Pb/^{238}U$ microprobe geochronology by the monitoring of a trace-element-related matrix effect; SHRIMP, ID–TIMS, ELA–ICP–MS and oxygen isotope documentation for a series of zircon standards. Chem. Geol. 205, 115–140.

Bouvier, A., Vervoort, J.D., Patchett, P.J., 2008. The Lu–Hf and Sm–Nd isotopic composition of CHUR: Constraints from unequilibrated chondrites and implications for the bulk composition of terrestrial planets. Earth Planet. Sci. Lett. 273, 48–57.

Bowring, J.F., McLean, N.M., Bowring, S.A., 2011. Engineering cyber infrastructure for U-Pb geochronology: Tripoli and U-Pb_Redux. Geochem. Geophys. Geosyst. 12, Q0AA19.

Condon, D.J., McLean, N., Schoene, B., Bowring, S., Parrish, R., Noble, S., 2008. Synthetic U-Pb "standard" solutions for ID-TIMS geochronology. Geochimica et Cosmochimica Acta 72 Supplement, 175.

de Saint Blanquat, M., Horsman, E., Habert, G., Morgan, S., Vanderhaeghe, O., Law, R., Tikoff, B., 2011. Multiscale magmatic cyclicity, duration of pluton construction, and the paradoxical relationship between tectonism and plutonism in continental arcs. Tectonophysics 500, 20–33.

Dilles, J.H., Proffett, J.M., 1995. Metallogenesis of the Yerington batholith, Nevada, in: Pierse, F.W., Bolm, J.G. (Eds.), Porphyry Copper Deposits of the American Cordillera. Arizona Geological Society Digest, pp. 306–315.

Gerstenberger, H., Haase, G., 1997. A highly effective emitter substance for mass spectrometric Pb isotope ratio determinations. Chem. Geol. 136, 309–312.

Hiess, J., Condon, D.J., McLean, N., Noble, S.R., 2012. $^{238}U/^{235}U$ systematics in terrestrial uranium-bearing minerals. Science 335, 1610–1614.

Jackson, S.E. (2008). LAMTRACE data reduction software *for LA*-ICP-MS. In: Sylvester, P. (Ed.), Laser-Ablation-ICPMS in the Earth Sciences: current practices and outstanding issues: Mineralogical Association of Canada Short Course Series, 40, 305-307.

Jackson, S.E., Pearson, N.J., Griffin, W.L., Belousova, E.A., 2004. The application of laser ablation-inductively coupled plasma-mass spectrometry to in situ U–Pb zircon geochronology. Chem. Geol. 211, 47–69.

Krogh, T.E., 1973. A low-contamination method for hydrothermal decomposition of zircon and extraction of U and Pb for isotopic age determinations. Geochim. Cosmochim. Acta 37, 485–494.

Schoene, B., Guex, J., Bartolini, A., Schaltegger, U., Blackburn, T.J., 2010. Correlating the end-Triassic mass extinction and flood basalt volcanism at the 100 ka level. Geology 38, 387–390.

Steinberger, I., Hinks, D., Driesner, T., Heinrich, C.A., 2013. Source plutons driving porphyry copper ore formation: combining geomagnetic data, thermal constraints, and chemical mass balance to quantify the magma chamber beneath the Bingham Canyon deposit. Econ. Geol. 108, 605–624.

Ulianov, A., Müntener, O., Schaltegger, U., Bussy, F., 2012. The data treatment dependent variability of U–Pb zircon ages obtained using mono-collector, sector field, laser ablation ICPMS. J. of Analytical Atomic Spectrometry 27, 663–676.

Wiedenbeck, M., Allé, P., Corfú, F., Griffin, W.L., Meier, M., Oberli, F., vonQuadt, A., Roddick, J.C., Spiegel, W., 1995. Three natural zircon standards for U-Th-Pb, Lu-Hf, trace Element and REE analyses. Geostandards and Geoanalytical Res. 19, 1–23.

Wohlets, K. (2008) KWare-Geological software, HEAT3D, http://geodynamics.lanl.gov/Wohletz/Heat.htm#Download

Wotzlaw, J.-F., Bindeman, I.N., Schaltegger, U., Brooks, C.K., Naslund, H.R., 2012. High-resolution insights into episodes of crystallization, hydrothermal alteration and remelting in the Skaergaard intrusive complex. Earth Planet. Sci. Lett. 355-356, 199–212.

Wotzlaw, J.F., Schaltegger, U., Frick, D.A., Dungan, M.A., Gerdes, A., Günther, D., 2013.

Tracking the evolution of large-volume silicic magma reservoirs from assembly to supereruption. Geology in press.